September 2, 1994

Docket No. 50-255

Mr. Robert A. Fenech
Vice President, Nuclear Operations
Consumers Power Company
Palisades Plant
27780 Blue Star Memorial Highway
Covert, Michigan 49043

Dear Mr. Fenech:

SUBJECT: PALISADES PLANT - TRANSMITTAL OF TECHNICAL EVALUATION REPORT (M83227)

In our evaluation of Palisades pressurized thermal shock and reactor vessel integrity issues, an assessment of the Palisades pressure vessel and reactor cavity fluence estimates and the associated uncertainties was conducted by our consultant, Brookhaven National Laboratory (BNL). The assessment demonstrated that the your fluence calculation methodology renders conservative results with respect to the best estimate BNL calculations and is acceptable.

A copy of the BNL technical evaluation report is enclosed.

Sincerely,

Original signed by

Anthony H. Hsia, Project Manager
Project Directorate III-1
Division of Reactor Projects III/IV
Office of Nuclear Reactor Regulation

Enclosure:
Technical Evaluation Report

cc w/enclosure:
See next page

OFFICE	LA:PD31	PM:PD31	BC:SRXB	PD:PD31
NAME	LLessler	AHsia:gll	RJones	LMarsh
DATE	08/23/94	08/23/94	08/31/94	09/2/94

OFFICIAL RECORD COPY FILENAME: G:\WPDOCS\PALISADE\PA83227.TER

080012

MA4

DF01

Mr. Robert A. Fenech
Consumers Power Company

Palisades Plant

cc:

Mr. Thomas J. Palmisano
Plant General Manager
Palisades Plant
27780 Blue Star Memorial Highway
Covert, MI 49043

Mr. David W. Rogers
Plant Safety and Licensing Director
Palisades Plant
27780 Blue Star Memorial Highway
Covert, Michigan 49043

M. I. Miller, Esquire
Sidley & Austin
54th Floor
One First National Plaza
Chicago, Illinois 60603

Mr. Thomas A. McNish, Secretary
Consumers Power Company
212 West Michigan Avenue
Jackson, Michigan 49201

Judd L. Bacon, Esquire
Consumers Power Company
212 West Michigan Avenue
Jackson, Michigan 49201

Regional Administrator, Region III
U.S. Nuclear Regulatory Commission
801 Warrenville Road
Lisle, Illinois 60532-4351

Jerry Sarno
Township Supervisor
Covert Township
36197 M-140 Highway
Covert, Michigan 49043

Office of the Governor
Room 1 - Capitol Building
Lansing, Michigan 48913

U.S. Nuclear Regulatory Commission
Resident Inspector Office
Palisades Plant
27782 Blue Star Memorial Highway
Covert, Michigan 49043

Nuclear Facilities and Environmental
Monitoring Section Office
Division of Radiological Health
Department of Public Health
3423 N. Logan Street
P. O. Box 30195
Lansing, Michigan 48909

Gerald Charnoff, Esquire
Shaw, Pittman, Potts and Trowbridge
2300 N Street, N. W.
Washington DC 20037

Alora Davis
Commitment Tracking System
Coordinator
Palisades Plant
Consumers Power Company
27780 Blue Star Memorial Highway
Covert, Michigan 49043-9530

DISTRIBUTION FOR TECHNICAL EVALUATION REPORT: DATED: September 2, 1994

Docket File
NRC & LPDRs
PD31 Rdg File
JRoe
EAdensam
JZwolinski
LMarsh
AHsia
CJamerson
LLois, SRXB
RJones, SRXB
OGC
ACRS (10)
MParker, Palisades
WKropp, RIII

ENCLOSURE

BROOKHAVEN NATIONAL LABORATORY

MEMORANDUM

DATE: March 15, 1994

TO: L. Lois

FROM: J. F. Carew, K. Hu and A. Aronson

SUBJECT: Palisades Pressure Vessel and Cavity Fluence Evaluation

I. Summary

Detailed calculations of the Palisades pressure vessel and cavity fluence have been carried out. The calculations use a pin-wise fuel exposure dependent description of the core neutron source, and plant design and operating data provided by Westinghouse and Consumers Power. The calculations employ the latest available ENDF/B-VI cross sections for iron and water. The calculations indicate that the Westinghouse prediction of the vessel > 1-MeV inner-wall fluence is conservative by ~ 10% relative to the best-estimate BNL calculation of 1.41 x 10^{19} n/cm^2 at the end of Cycle-9. The (one-sigma) uncertainty in the BNL > 1-MeV fluence is estimated to be ~ ±17%.

II. Introduction

The recently released ENDF/B-VI nuclear data files include a significant reduction in the iron inelastic scattering cross section (Reference 1). The resulting reduced flux attenuation in the core barrel, thermal shield and in the vessel itself is expected to result in a substantial increase in the predicted vessel inner-wall and cavity fluences. The purpose of the present analysis is to (1) determine the effects of these cross section updates for pressure vessels with and without thermal shields and (2) evaluate the best-estimate fluence for the Palisades plant.

In performing this analysis a substantial effort was made to insure the use of the latest nuclear cross section and fission spectra data. The required plant operating and design data including (1) the geometry of the core, internals, vessel and cavity, (2) the cycle-dependent power and exposure distributions, (3) the operating temperatures, and (4) the parameter uncertainties were obtained from Consumers Power and Westinghouse. While this plant data was reviewed and generally found to be within expected limits, a detailed validation of this input data was not performed. A significant effort was made to update the MESH code (Reference-2) to allow an accurate modeling of the core pin-wise power and source distributions.

Pressure vessel fluence calculations were performed for both the Palisades plant, which does not include a thermal shield, and a second PWR plant including a thermal shield. The calculations were performed using both ENDF/B-IV and ENDF/B-VI cross sections and fission spectra. The DORT discrete ordinates transport code (Reference-3) was used to calculate the transport of the core neutron flux out to the vessel and into the cavity. The DORT calculations were performed for an axially-averaged horizontal plane in (r,θ) geometry. The MESH code was used to determine the space-energy dependent core neutron source in the required (r,θ) geometry for input to DORT. Cycle-specific DORT calculations were performed and combined to determine the total accumulated vessel fluence. The best-estimate vessel fluence and calculation uncertainties and biases were compared to the Westinghouse Cycle-9 predictions for Palisades (Reference-4). In addition, the ENDF/B-IV to ENDF/B-VI fluence bias for plants with and without thermal shields was determined.

The details of the calculation methods used to perform these analyses are described in Section-III and the results of the fluence analyses are provided in Section-IV.

III. Calculational Methodology

III.1 Neutron Cross Sections and Fission Spectra

The Palisades fluence calculations were performed with both the base and an updated version of the 47-group SAILOR cross section library. The base SAILOR (Reference-5) library was determined by collapsing the ENDF/B-IV VITAMIN-C (Reference-6) 171-group cross section set using spatially dependent spectra calculated for a typical PWR configuration. The SAILOR library update was necessary for the benchmark calculations in order to include the ENDF/B-VI versions of the iron, hydrogen and oxygen cross sections, which are known to have a significant effect on pressure vessel fluence predictions. The ENDF/B-VI cross sections for these isotopes were obtained from RSIC and combined with the base SAILOR library to form the update.

The fission spectra for U-235, U-238, Pu-239, Pu-240, Pu-241, and Pu-242 were used in the MESH calculations of the core neutron source. The ENDF/B-VI fission spectra for U-235, U-238, Pu-239 and Pu-241 were processed with NJOY (Reference-7) and calculations were performed with both the ENDF/B-VI and base spectra used in the Palisades analysis. These calculations indicated that the >1-MeV and >0.10 MeV fluences agreed to within $\lesssim 1.0\%$.

The capsule dosimeter reaction rates were calculated using ENDF/B-VI cross sections. The cross section data were collapsed to the 47-group structure using NJOY.

III.2 Core Neutron Source

The calculation of the core neutron source includes the effect of the strong pin-wise variations of the power distribution in the fuel assemblies located near the core boundary. The

MESH code was used to allocate the pin-wise power to the individual (r, θ) mesh blocks. This allocation was performed by a numerical integration of the power distribution, defined on the (x, y) pin-wise mesh, over each (r, θ) mesh block. This numerical integration typically employed > 100 integration mesh per fuel pin and was shown to be accurate to within $\lesssim 1\%$ for each (r,θ) mesh block. As examples, the detailed core neutron source for Cycle-9 of Palisades and for the initial cycle of Plant-TS are given in Figure-1 and Figure-2, respectively.

The magnitude of the core neutron source increases with fuel burnup due to the higher number of neutrons produced per MeV of energy by a Pu fission. This was taken into account by calculating the number of neutrons per MeV, ν/κ [neutrons/MeV], using the fuel burnup dependent isotopic fission fractions. In addition, the fission spectrum was also considered to be dependent on the fuel burnup in order to account for the harder more penetrating neutron spectrum characteristic of the Pu fissions in the high burnup fuel.

III.3 Neutron Transport Calculations

The neutron transport calculations were performed with the ORNL DORT discrete ordinates transport code using the 47-group SAILOR library, modified to include the ENDF/B-VI iron, oxygen and hydrogen cross sections. The calculations were performed in a fixed source mode for a radial (r,θ) plane. The radial (r,θ) calculations were performed in a two-step "boot strap" fashion in which an inner one-eighth 45° azimuthal sector was first calculated. A second outer one-eighth core 45° annular sector was then calculated using the flux on the inner surface of the annulus, calculated in the first inner calculation, as an input boundary condition. A ~ 15 cm radial overlap-region between the inner and outer calculations was maintained to insure that the neglect of the outer geometry in the inner problem had a negligible effect ($\lesssim 0.5\%$) on the vessel fluence calculations. The vessel axial peak for the Palisades and Plant-TS fluence calculations was conservatively taken to be the same as the core peripheral axial power peak.

The calculations were performed using an S_8 quadrature and a P-3 angular decomposition of the scattering cross sections. The (r,θ) mesh included 61(67) angular mesh intervals, and 106(123) and 100(63) radial mesh intervals in the inner and outer Palisades (Plant-TS) bootstrap calculations, respectively. The angular (θ) and radial (r) mesh densities were increased at material interfaces where the geometry was changing rapidly and at the capsule locations.

Vacuum boundary conditions were used on the outer radial and axial boundaries of the problems and reflecting boundary conditions were used on the internal $\theta = 0°$ and $\theta = 45°$ azimuthal boundaries. A pointwise flux convergence of 10^{-3} was used together with an integrated flux convergence criteria of 10^{-3}.

IV. Vessel Fluence Analysis

IV.1 Palisades Fluence Calculations

The calculated Palisades Fluence is presented in Table-1 and indicates a peak > 1-MeV fluence of 1.524 x 10^{19} n/cm^2 at the vessel inner-wall at the end of Cycle-9. The fluences for Cycles 1-5 and for Cycles 6 and 7 have been combined and are provided in Table-1. For comparison, the Westinghouse predictions of the cycle-dependent fluences are also presented and indicate a 3% overprediction relative to the BNL calculation.

The Westinghouse calculation includes certain approximations which are known to introduce a bias into the inner-wall fluence predictions. In Table-2, the effects of these biases are presented. The effect of updating the ENDF/B-IV data to the latest ENDF/B-VI iron, hydrogen and oxygen cross sections is given in Columns 1 and 2. In these calculations the iron in the baffle, barrel, vessel, PV insulation and concrete biological shield was updated to ENDF/B-VI. The hydrogen and oxygen in the core, reactor coolant, PV insulation, cavity and concrete biological shield were also updated to ENDF/B-VI. The reduced iron scattering cross section increases the fluence by ~4.6%, while the hydrogen and oxygen ENDF/B-VI cross sections reduce the fluence by ~2.7%. The major effect of the cross section update was due to the baffle, barrel and vessel iron and the hydrogen and oxygen in the coolant. The effect of updating the noncoolant hydrogen and oxygen cross sections was small and had the following effect: (1) updating the core H_2O cross sections decreased the inner-wall > 1-MeV flux by ~1%, (2) updating the cavity oxygen insulation and air cross sections decreased the > 1-MeV flux throughout the cavity by ~0.2% and (3) updating the biological shield concrete iron, oxygen and hydrogen cross sections decreased the > 1-MeV flux throughout the cavity by 0.2%. In Column-3, the effect of the reduced cooler temperature in the peripheral assemblies (relative to the core average) is seen to reduce the vessel fluence by ~1.5%. The effect of using the core-average temperature between the baffle and barrel is given in Column-4, and the effect of thermal expansion is given in Column-5. The effect of updating to the ENDF/B-VI fission spectra is given in Column-6 and is seen to be ~1%. The net effect of all these approximations is to reduce the Palisades Cycle-9 > 1-MeV fluence by ~7%. The BNL calculated fluence including these (seven) adjustments is given in Table-3 and shows that the Cycle-9 Westinghouse fluence is ~10% higher than the BNL best-estimate prediction.

In order to estimate the uncertainty in the BNL > 1-MeV fluence prediction, a series of sensitivity calculations were performed for the known sources of significant uncertainty. In Table-4, these sensitivities are given along with the estimated (one-sigma) uncertainty components. The pressure vessel diameter uncertainty of ± 0.33 in. was provided by Consumers Power (Reference-8). The 8% source uncertainty (Item-2) is based, in part, on an estimate of the uncertainty in the peripheral assembly powers, and the (Item-5) water temperature uncertainties are based on expected reactor coolant system temperature calculation/measurement uncertainties. The nuclear data uncertainty estimate (Item-3) is based on expected data uncertainties and the numerical procedures uncertainty (Item-4) is based on sensitivity and modeling calculations. The other uncertainties included in Item-6 are relatively

small model uncertainties that combine to add an additional 5% uncertainty to the total fluence. The total Palisades inner-wall > 1-MeV fluence uncertainty estimate is ± 17% (one-sigma).

IV.2 Effects of a Thermal Shield

The increase in vessel fluence resulting from the reduced ENDF/B-VI iron scattering cross sections depends on the thickness of steel between the core and the vessel. The Palisades plant has no thermal shield and, consequently, plants having a thermal shield are expected to have a larger fluence increase than the 4.6% increase calculated for Palisades (Column-1, Table-2). In order to determine the fluence increase resulting from the updated ENDF/B-VI cross sections a Plant-TS with a thermal shield was also calculated.

In Table-5, the > 1-MeV flux predictions for the first cycle of plant-TS are presented. For comparison, the corresponding Westinghouse predictions are also presented and indicate slight underpredictions (relative to BNL) of 1.2% and 2.6% (rms over all angles) at the thermal shield $\theta = 0°$ outer-wall and cavity locations, respectively. Both the BNL and W predictions are based on the same assumptions concerning coolant temperatures, ENDF/B-IV nuclear data and thermal expansion. This good agreement is consistent with the BNL/W comparisons of Table-1. The effect of updating the nuclear data from ENDF/B-IV to the latest ENDF/B-VI iron, oxygen and hydrogen cross sections on the calculated fluxes is given in Table-6. In these calculations the iron in the baffle, barrel, thermal shield, vessel, PV insulation and concrete biological shield were updated to ENDF/B-VI. The hydrogen and oxygen in the core, reactor coolant, PV insulation, cavity and concrete biological shield were also updated to ENDF/B-VI. It is seen that for this plant, the > 1-MeV flux is increased by ~ 8.7% at the inner-wall and by ~ 31% in the cavity due to the updating of the cross section data. The corresponding increases for Palisades were ~ 1.8% and 21%, respectively.

In Table-7, the calculated reaction rates and fluxes are given for the Plant-TS capsule located on the outer wall of the thermal shield (at a radius of 211.41 cm and an azimuth of θ = 40°). The calculated and measured > 1-MeV fluxes are seen to agree within ~ 4% and the calculated reaction rates agree with the measurements to within ~ 17%.

JFC/ns

c: R.A. Bari (BNL)
M.A. Caruso (NRC)
C.L. Snead, Jr. (BNL)
B.E. Thomas (NRC)
G.J. Van Tuyle (BNL)

References

1. M. L. Williams, C. Aboughantous, M. Asgari, J. E. White. R. Q. Wright, and F. B. K. Kam, "Transport Calculations of Neutron Transmission Through Steel using ENDF/B-V, Revised ENDF/B-V and ENDF/B-VI Iron Evaluations," Annals Nuclear Energy, Vol. 18, No. 10, pp. 549-565, 1991.

2. "MESH - A Code for Determining the DOT Fixed Neutron Source," BNL-Memorandum, M. D. Zentner to J. F. Carew, August 25, 1981.

3. "DORT, Two-Dimensional Discrete Ordinates Transport Code," RSIC Computer Code Collection, CCC-484, Oak Ridge National Laboratory, 1988.

4. "Palisades Fluence Data," Letter, E. P. Lippincott (W) to J. F. Carew (BNL), dated October 27, 1992.

5. "SAILOR: Coupled, Self-Shielded, 47-Neutron, 20 Gamma-Ray, P3, Cross-Section Library for Light Water Reactors," RSIC Data Library Collection DLC-076, 1985.

6. "VITAMIN-C: 171 Neutron, 36 Gamma-Ray Group Cross Sections in AMPX and CCCC Interface Formats for Fusion and LMFBR Neutronics," RSIC Data Library Collection, DLC-41, 1978.

7. R. E. MacFarlane, D. W. Muir, and R. M. Boicourt, "The NJOY Nuclear Data Processing System, Volume I: User's Manual," LA-9303-M, Vol. I (ENDF-324), May 1982.

8. "Response to NRC Telecon Request," CPCO to L. Lois (NRC), dated July 12, 1993.

Figure 1

PALISADES CY 9 INNER REGION SOURCE

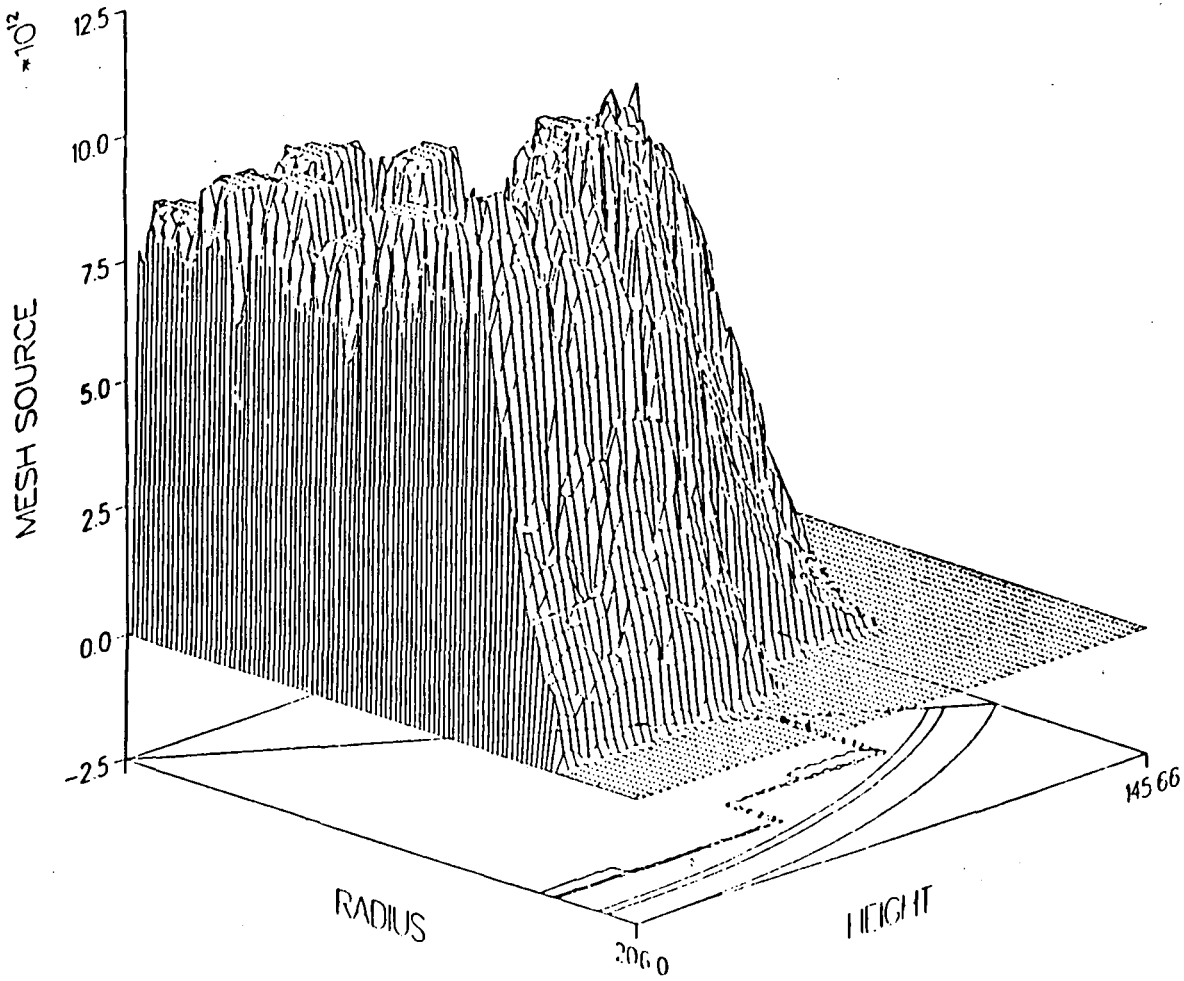

Figure 2

PLANT-TS INNER REGION SOURCE

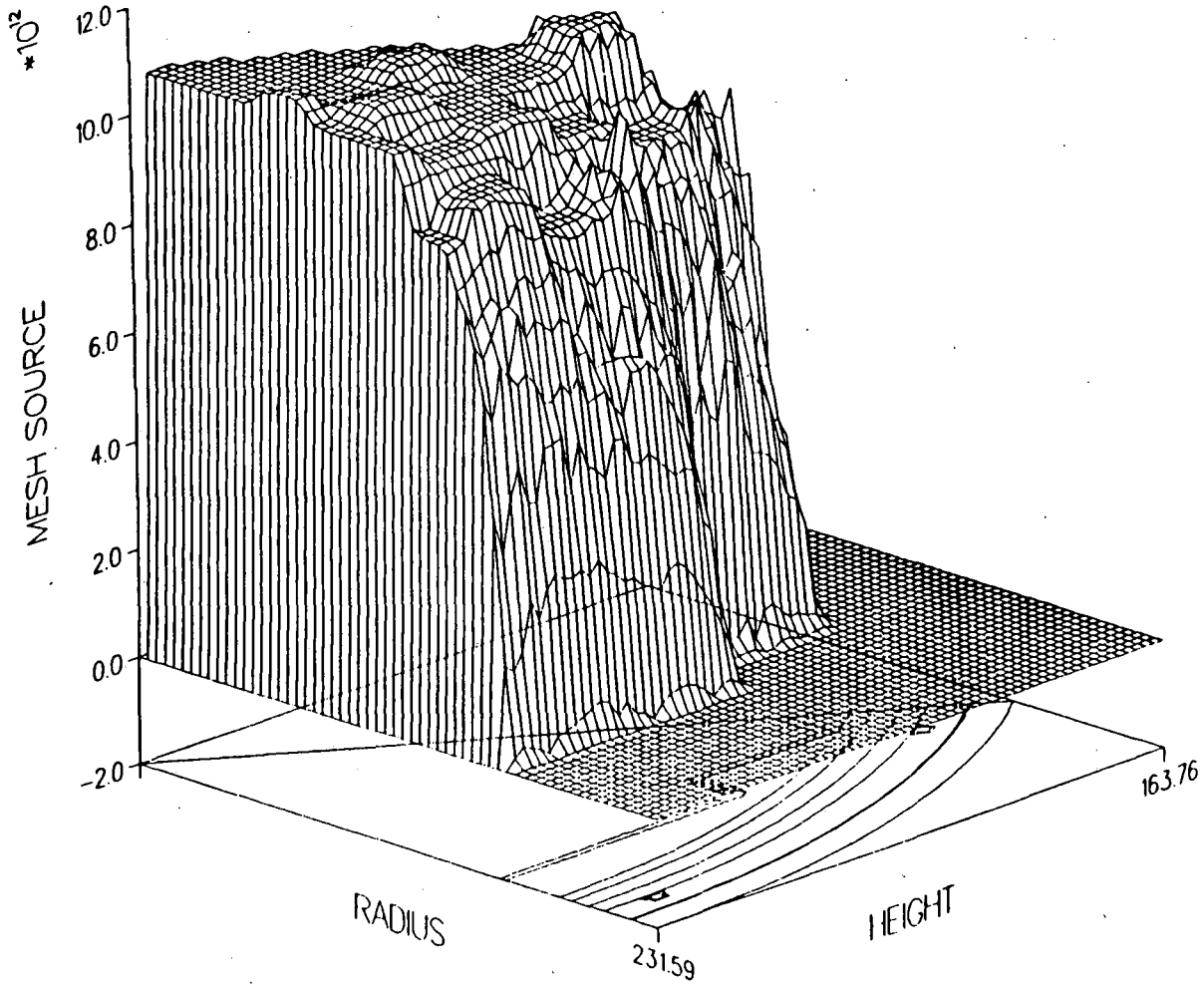

Table-1

Comparison of BNL and Westinghouse Palisades Fluence Calculations at Pressure Vessel Inner Wall Peak (E > 1.0MeV)

Cycle	Cycle Length (sec)	Fluence** (neutron/cm**2)		Ratio*
		W	BNL	
1-5	1.6417728×10^{8}	9.68042×10^{18}	9.25288×10^{18}	0.956
6-7	6.076512×10^{7}	3.71556×10^{18}	3.66116×10^{18}	0.985
8	3.227904×10^{7}	1.50198×10^{18}	1.52399×10^{18}	1.015
9	2.628288×10^{7}	7.83419×10^{17}	7.97646×10^{17}	1.018
Total	2.8350432×10^{8}	1.56814×10^{19}	1.52357×10^{19}	0.972

* Ratio = Fluence (BNL)/Fluence (W)

** Fluences were taken at maximum azimuth

Table-2

BNL Palisades Fluence Calculation Adjustments

Cycle	% - Adjustments							
	(1)	(2)	(3)	(4)	(5)	(6)	(7)	Total
1-5	4.6	-2.70	-1.3	-5.4	-2.35	1.0	-1.1	-7.25
6-7	4.6	-2.70	-0.8	-5.0	-2.35	1.0	-1.1	-6.35
8	4.6	-2.70	-2.7	-6.0	-2.35	1.0	-1.1	-9.25
9	4.6	-2.70	-3.4	-6.6	-2.35	1.0	-1.1	-10.55
Total* 1-9	4.6	-2.70	-1.43	-5.42	-2.35	1.0	-1.1	-7.40

(1) Iron cross section based on ENDF/B-VI.

(2) Hydrogen and Oxygen cross sections based on ENDF/B-VI.

(3) Peripheral assembly water temperature lower than the core average temperature.

(4) Water temperature between baffle and barrel lower than the core average temperature.

(5) Water thickness between core and pressure vessel is based on the hot condition.

(6) ENDF/B-VI fission spectra were used.

(7) Axial Leakage was corrected.

* Total adjustments are based on the contribution of each cycle to the total accumulated fluence (Cycles 1-5 = 61%, Cycles 6-7 = 24%, Cycle 8 = 10%, Cycle 9 = 5%)

Table-3

Comparison of Adjusted BNL and Westinghouse Palisades Fluence Calculations at Pressure Vessel Inner Wall Peak (E > 1.0MeV)

Cycle	Cycle Length (sec)	Fluence** (neutron/cm**2)		Ratio*
		W	BNL	
1-5	1.6417728×10^{8}	9.68042×10^{18}	8.58205×10^{18}	0.887
6-7	6.076512×10^{7}	3.71556×10^{18}	3.42868×10^{18}	0.923
8	3.227904×10^{7}	1.50198×10^{18}	1.38302×10^{18}	0.921
9	2.628288×10^{7}	7.83419×10^{17}	7.13494×10^{17}	0.911
Total	2.8350432×10^{8}	1.56814×10^{19}	1.41072×10^{19}	0.900

* Ratio = Fluence (BNL)/Fluence (W)
** Fluences were taken at maximum azimuth

Table-4

BNL Palisades Fluence Calculation Uncertainty Analysis

Uncertainty Source	Fluence Sensitivity	Estimated Uncertainty	Fluence Uncertainty
1. PV Diameter	32%dF/in	+0.33 in	+10.6%dF
2. Core Neutron Source	1.0%dF/%ds	+8%ds	+8%dF
3. Nuclear Data			+7%dF
4. Numerical Procedures			+6%dF
5. Water Temperature:			
Core	0.25%dF/°F	+4°F	+1%dF
Bypass	0.37%dF/°F	+9°F	+3.33%dF
Down Comer	0.36%dF/°F	+4°F	+1.44%dF
6. Others			+5.0%dF
Total			+17.3%

Table-5

Plant-TS Thermal Shield & Cavity Capsule Fluxes (E > 1.0 MeV)
($n/cm^2 \cdot sec$)

	Thermal Shield r=211.41cm	Cavity r=252.39cm			
	θ=40°	θ=0°	θ=13.5°	θ=33.8°	θ=45°
BNL(B-IV)*	6.71×10^{10}	2.74×10^{8}	3.94×10^{8}	5.91×10^{8}	6.54×10^{8}
W(B-IV)	6.63×10^{10}	2.63×10^{8}	3.83×10^{8}	5.85×10^{8}	6.53×10^{8}
$\%\Delta\phi$**	+1.2	+4.2	+2.9	+1.0	0

* B-IV corresponds to ENDF/B-IV.
** $\%\Delta\phi$ = [BNL(B-IV) - W(B-IV)] x 100/W(B-IV).

Table-6

Effect of Updating The Cross Sections From ENDF/B-IV to ENDF/B-VI
Pressure Vessel & Cavity Fluxes (E > 1.0 MeV)

	BNL (B -IV)*	BNL (B-VI)	%Δφ**
	(n/cm^2 · sec)		
Palisades Inner Wall r=219.393cm θ=15.5°	3.03485x10^{10}	3.08835x10^{10}	+1.8
Palisades Cavity r=332.105 θ=15.5°	8.02819x10^{8}	9.71525x10^{8}	+21.0
Plant-TS Inner Wall r=220.635cm θ=18°	1.12550x10^{10}	1.22380x10^{10}	+8.7
Plant-TS Cavity r=252.39cm θ=18°	4.45996x10^{8}	5.84394x10^{8}	+31.0

* B-IV corresponds to ENDF/B-IV.
** %Δφ = [BNL(B-VI)-BNL(B-IV)] x 100/BNL(B-IV).

Table-7

Plant-TS Thermal Shield Capsule
Flux (E > 1.0 MeV) and Reaction Rates
(r = 211.41cm, θ = 40°)

	W (measurement)	BNL (B-IV)*	W (B-IV)	BNL (B-VI)	$\%\Delta\phi$**
63 Cu (n,a)	4.89×10^{-17}	4.18×10^{-17}	4.58×10^{-17}	4.60×10^{-17}	-5.9
54 Fe (n,p)	4.39×10^{-15}	4.49×10^{-15}	4.41×10^{-15}	5.12×10^{-15}	+16.6
58 Ni (n,p)	7.10×10^{-15}	6.24×10^{-15}	5.92×10^{-15}	7.07×10^{-15}	-0.4
238 U (n,f)	2.69×10^{-14}	2.32×10^{-14}	2.22×10^{-14}	2.57×10^{-14}	-4.5
237 Np (n,f)	2.14×10^{-13}	1.84×10^{-13}	1.84×10^{-13}	2.01×10^{-13}	-6.1
Flux(E > 1.0MeV) ($n/cm^2 \cdot sec$)	$7.67 \times 10^{+10}$	$6.71 \times 10^{+10}$	$6.63 \times 10^{+10}$	$7.39 \times 10^{+10}$	-3.7

* B-IV corresponds to ENDF/B-IV.
** $\%\Delta\phi$ = [BNL (B-VI) -W (measurement)] x 100/W (measurement).